Elevated pressure and temperature effect to laminar flame speed of acetone/air mixture

Yi Wu, Vincent Modica, Frédéric Grisch
CORIA-UMR 6614- Normandie Université, CNRS-Université et INSA de Rouen
Campus Universitaire du Madrillet, 76800, Saint-Etienne du Rouvray, France

1. Introduction

Acetone is not only important as an intermediate produced in hydrocarbon oxidation, but is also of interest since it is used as fuel tracer in laser induced fluorescence measurements [1] [2]. The fuel tracer added into the combustible should not disturb the reactive flow. A well understanding of the combustion characteristics can be used to evaluate the usefulness of acetone as a fuel tracer, among which laminar flame speed is one of the most essential physical properties. In recent years, laminar flame speed of acetone/air has been studies by various previous investigations [3] [4] [5]. In Cheng et al's work [6], laminar flame speed of acetone/air was measured by particle imaging velocimetry technique using a jet-wall stagnation flame with temperature 300K and ambient pressure condition. Acetone/air flame speed was measured in high temperature condition in E.J.K Nilsson's work [4] using a perforated plated burner at 0.1 MPa and initial gas mixture temperatures of 298K-358K. Other fundamental physical properties such as ignition delays, species measurement in acetone flame can be found in S.Pichon et al's work [5]. However, limited experimental measurements were performed in higher pressure and high temperature greater than 400K. Thus, there are still interests to learn the laminar flame speed of acetone/air and its combustion behavior in high pressure and high temperature conditions to adapt optic diagnostic applications as a fuel tracer. In this work, laminar flame speed of acetone/air was measured by a Bunsen liked burner in high temperature T=373K to 468K and high pressure 0.1MPa to 0.5MPa over a large equivalence ratios range. From these experimental data, temperature and pressure dependency correlation formulation of laminar flame speed is proposed and compared with numerical simulation results.

2. Experimental set-up and methodology

The experiment set-up consisted of a converged nozzle Bunsen burner in a stainless steel high pressure chamber, heated gas feeding lines, a liquid fuel vaporization system and optic diagnostic image acquisition system. As shown in figure 1 the bottom of the burner is a cylinder with a diameter 100mm and converged to a diameter 10mm at exit of the nozzle. The contoured nozzle burner has a sintered plated (diameter 10.6mm) stabilized pilot flame around the rim of the nozzle exit to stabilize the main jet flame. This becomes necessary in high pressure and lean equivalent ratio working conditions as the static

Correspondence to:yi.wu@coria.fr

stability (flash back, blow off and thermos acoustic instability) of the jet flame stabilized on a contoured nozzle is limited to a narrow range of operating velocities. The whole burner is placed in a high pressure chamber (height 520mm and diameters 100 x 100mm) with three optic accesses.

All the flow line and the whole chamber were preheated to working temperature by electrical resistance tape and circulation heater. The co-flow nitrogen was delivered to the chamber by a flow controller in order to get high pressure combustion environment in the chamber. The reactant temperature was monitored by a temporary placed thermocouple in the exit of the burner. Once the desired temperature achieved the surface temperature of the chamber and circulation heaters will be held constant by temperature controllers. The pressure in the chamber was controlled by different diameters sonic nozzle located at the downstream of the chamber. This high pressure chamber is designed to withstand pressure up to 3Mpa and temperature up to 600K.

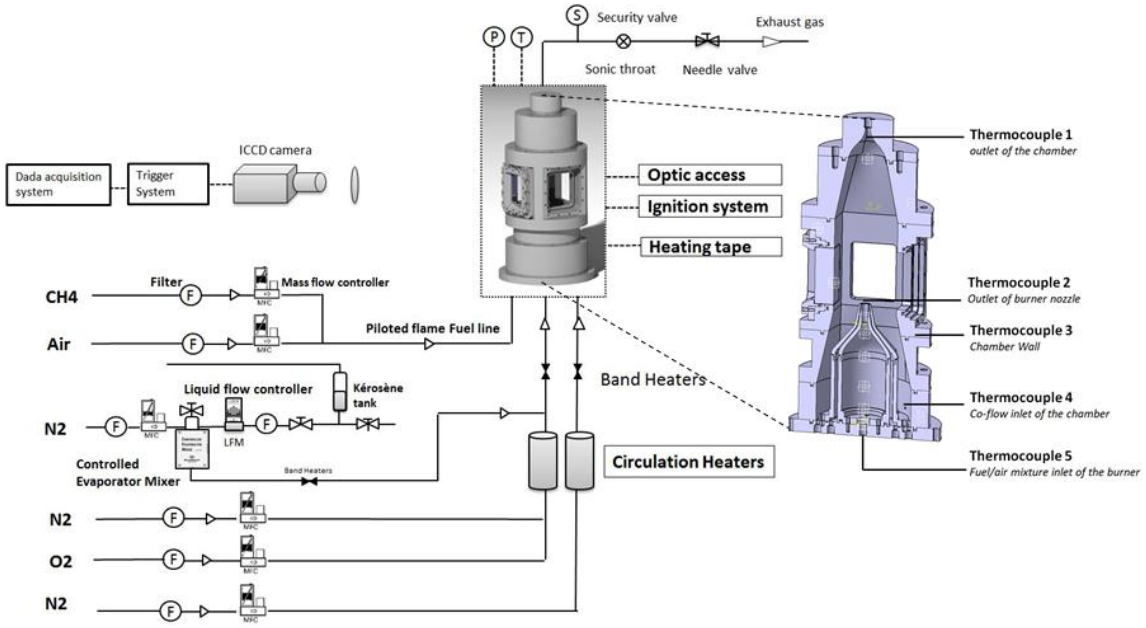

Fig.1. schematic of the experimental facility dedicated to premixed acetone/air combustion

Bunsen flame is one of the most used to learn laminar flame speed [7] [8] [9], assuming that the burning velocity is the same over the entire surface area the flame, the flame speed can be calculated applying mass conservation balance as equation 1. With ρ_u, the unburned gas density and Q_m the total mass flow rate of the fuel/air mixture gas. This method requires a knowledge of the entire surface area A, deduced in the present investigation by analyzing OH* chemiluminescence images of the flames. An image processing algorithm was developed by using Abel inversion to get the outside maximum intensity contours. According to the definition of flame speed, it's the velocity relative to unburned gas which is not corresponded with maximum OH* contours. OH* maximum point locates almost in the end of the combustion process. The flame speed could be underestimated if the maximum OH* surface is used. For this reason, a correction reference surface needs to be defined. In this work, the reference surface was calculated via shifting the maximum OH* surface by a 'flame thickness' defined as $\delta=X_{T=800K}-X_{[OH]max}$, which begins at the temperature 800 K and ends at the maximum chemiluminescence [OH]*. Temperature 800K was used because generally the OH* begins to appeared at this temperature in early combustion

zone (preheat up stream). This defined flame thickness is calculated by 1D adiabatic premixed flame temperature and OH profiles from numerical simulation.

$$\rho_u S_u A = Q_m \rightarrow S_u = \frac{Q_m}{\rho_u * A} \qquad \text{Eq.1}$$

3. Numerical method

Experimental results are compared to numerical calculated one dimension adiabatic no-stretched flame speed values using published chemical kinetic mechanism by software COSILAB. Methane chemical kinetic mechanism GRI Mech 3.0 was used for CH4/air flame speed calculation. A sub-mechanism consisted by acetone oxidation and pyrolysis reactions are added to GRI Mech 3.0 to simulate acetone/air flame speed. Kinetic mechanism details of acetone/air used in present work can be found in Cheng et al.'s work. [6]

4. Temperature effect

The first measurement of laminar flame speed was performed using CH4/air to validate the system measurement accuracy in comparing with previous experimental measurements from literatures and numerical simulation results using GRI-Mech 3.0. For an equivalence ratio range of 0.7-1.4, temperature 300K and ambient pressure condition in figure 2a, a good agreement was observed comparing with previous experimental works as well as numerical simulations which suggests the accuracy of our measurement system and image processing algorithm. There is a slight discrepancy for richer equivalent ratio side where the simulated flame speed is greater than experimental measurement results.

To learn initial temperature effect to acetone/air laminar flame speed, experimental measurements were performed in four different temperatures. Experimental and modeling results were shown in figure 2b at elevated initial gas mixture temperature: 373K, 403K, 443K and 468K. Experimental and modeling results are in good agreement on the lean side. On the equivalence ratio richer part, however it shows a discrepancy that experimental measurements are overestimated compared with simulation results. The discrepancy could be caused by the fresh fuel/air mixtures temperature augmentation due to the heat generated by the flame, as the image acquisition was proceeded in a continuous way from φ=0.6 to φ =1.4. As shown in figure 2 that the laminar flame speeds were observed to increase with the fuel/air mixtures temperature. The temperature dependence correlation of laminar flame speed, which only has been investigated by limited previous work for acetone/air flame, was proposed in this work. The most widely used correlation is represented by Eq. (2). This is a generalized correlation that gives the laminar flame speed in terms of pressure, unburned mixture temperature, and equivalence ratio.

$$S_u = S_{u0}(\varphi)\left(\frac{T}{T_0}\right)^{\alpha}\left(\frac{P}{P_0}\right)^{\beta} \qquad \text{(Eq.2)}$$

$$S_{u0}(\varphi) = S_{u_0,\varphi=1} + S_{u_0,1}(\varphi-1) + S_{u_0,2}(\varphi-1)^2 + S_{u_0,3}(\varphi-1)^3 + S_{u_0,4}(\varphi-1)^4 \qquad \text{(Eq.3)}$$

$$\alpha(\varphi) = \alpha_0 + \alpha_1(\varphi-1) + \alpha_2(\varphi-1)^2 + \alpha_3(\varphi-1)^3 \qquad \text{(Eq.4)}$$

Where S_{u0} is the flame speed at reference condition and here the effect of equivalence ratio is taken into account in Eq. (3) by using an extended formulation of Metghalchi and Keke [10]. T_0, P_0 is the reference temperature and pressure. $S_{u_0,\varphi=1}$ is the laminar flame speed at φ=1 and $S_{u_0,i}$ the parameters to be determined for initial temperature T_0 of 373K and pressure P_0 of 0.1Mpa. The values of $S_{u_0,i}$ obtained

experimentally in this work are listed in table 1. It is a widely held view that the power exponent α depends on equivalence ratio. The power exponent α derived from experimental results in this work was plotted in figure 3(a) together with corresponding results calculated from Cosilab numerical simulation results and with previous results from the literatures. In figure 3(a), the results show a closed agreement with numerical simulation results and a minimum power exponent value was located at slightly rich mixtures (about 1.05). The calculated power exponents in this work were observed greater than previous E.J.K et al's experimental work, while the variation trend versus equivalent ratios has a good agreement. The dependency of α to equivalence ratio φ was derived by formulation Eq.4, the value of α_i obtained in current work is listed in table 1.

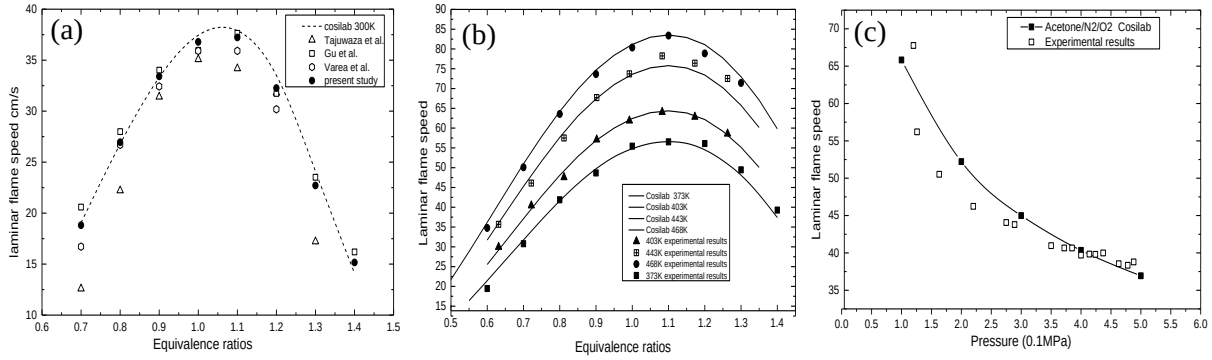

Fig.2. (a) Laminar flame speed S_u comparison between experimental measurements and previous literature results as well as with simulated results using GRI-Mech 3.0 (CH4/air, T_{air}=300K, P=0.1MPa). (b) Laminar flame speed of acetone/air at ambient pressure and different initial temperatures. Symbols represent experimental data, lines are modelling results (T=373K, 403K, 443K and 468K). (c) Comparison between experimental results and Cosilab simulation results acetone/air laminar flame speed versus pressure variation in T=473K, φ=0.8, P=0.1MPa -0.5MPa.

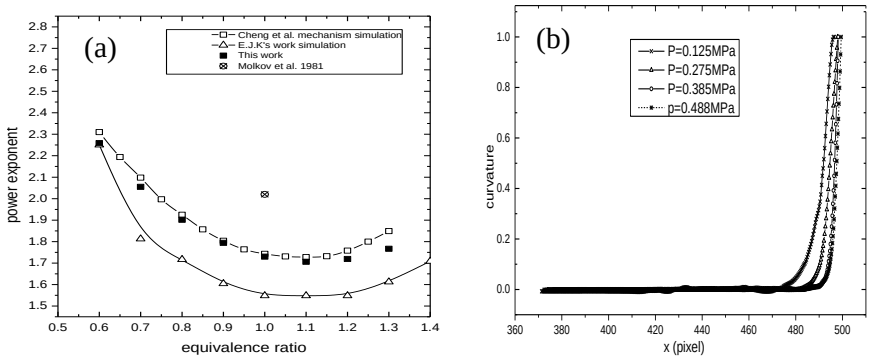

Fig.3. (a) Temperature power exponent coefficient α in Eq. 2 for acetone/air flames. (b) Normalized flame curvature rate along radius direction for different pressure 0.1Mpa to 0.5Mpa, T=473K, φ=0.8. Burner rim starts at pixel=370 pixel and burner center position 500 pixel.

$S_{u_0,\varphi=1}$	54.8
$S_{u_0,1}$	39.4
$S_{u_0,2}$	-161.9
$S_{u_0,3}$	-91.4
$S_{u_0,4}$	14.4

Table 1: Correlation parameters $S_{u_0,i}$ from Eq.3

α_0	1.73	β_0	-0.318
α_1	-0.44	β_1	-0.013
α_2	2.01	β_2	-0.889
α_2	-0.50	β_3	-0.371

Table2: correlation parameters α_i in Eq.4 (obtained by experimental results) and β_i in Eq.5 (obtained by simulation).

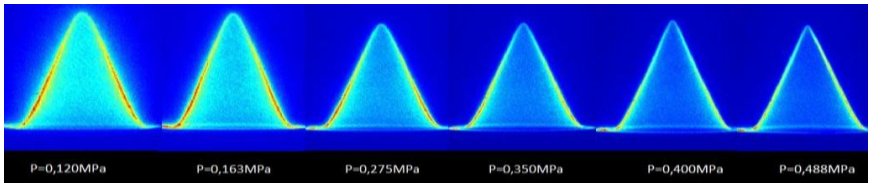

Fig. 4. Laminar flame structure of acetone/air versus pressure variation P=0.1-0.5MPa, ∅ =0.8, T=473K

5. Pressure effect

Laminar flame speed measurements were prospectively performed in different pressure P= 0.1MPa to 0.5 MPa with equivalence ratio 0.7-1.1 at an initial temperature 473K for pressure effects study. In figure 4 the flame structure variation were shown from 0.1Mpa to 0.5MPa for same equivalence ratio 0.8 and temperature 473K. It can be found that the flame top cusps become smaller and sharper in higher pressure compared with lower pressure. For a Bunsen liked flame, the condition of a constant burning velocity is violated at the top of the flame that additional influences such as flame curvature must be taken into account which is generally considered as the main source of flame stretch for a stationary Bunsen flame. The curvature variation along radius was plotted for different pressure in figure 3b. Flame stretch is manifested through the curvature along the flame surface, attaining its maximum value at the tip. The figure 4 shows that for lower pressure flame, the waist part (straight part) of the flame ends earlier and the alleviative curvature variation was observed. While for higher pressure, the whole flame surface is almost located at the waist part, there is a strong curvature gradient was appeared in a short radial distance which indicated a finer stretch effects to experimental flame speed determination.

$$\beta(\varphi) = \beta_0 + \beta_1(\varphi - 1) + \beta_2(\varphi - 1)^2 + \beta_3(\varphi - 1)^3 \quad \text{Eq.5}$$

Experimental results of laminar flame speed of acetone/air was shown in figure 2c in a variation of pressure, a higher pressure leads to a decrease of flame speed. The change in flame speed at lower pressure 0.1MPa to 0.3 MPa is more noticeable in this domain, at higher pressure levels 0.3MPa to 0.5MPa leads to smaller flame speed variation. This is also in agreement with the literature where the influence of pressure on laminar flame speed was numerically investigated for higher pressure, whilst the flame speed becoming almost constant for pressure higher than 0.8MPa. Comparing with the numerical simulation accomplished in this work, it is found that the numerical simulation give a higher flame speed comparing with empirical results from 0.1MPa to 0.3MPa and a better accordance in 0.3MPa to 0.5Mpa. The whole trend shows a good agreement with literature and simulation results as well. As shown in Eq.2 pressure dependency power exponent β was proposed in considering the equivalence ratio effects by formulation Eq.5. The value of β_i obtained by C.T. Chong's model simulation was present in table 2. Experimental results for β (φ=0.7) =-0.370, β (φ=0.8) =-0.325, β (φ=0.9) =-0.301 remains similar with simulation results -0.399, -0.359 and -0.331. A general correlation is then obtained to express the effect of pressure, temperature and equivalence ratio.

6. Conclusion

Laminar flame speed of acetone/air was measured by using Bunsen flame at unburned mixture temperature 373-473K and pressure conditions 0.1-0.5MPa over equivalence ratio 0.7-1.3. The results show a good agreement with simulation results and with previous literatures. The effects of initial fuel/air mixture temperature and pressure on the laminar flame speed were interpreted using the general correlation $S_u = S_{u0}(\varphi)(T/T_0)^{\alpha}(P/P_0)^{\beta}$. Particular attention has been paid to effect of equivalence ratio on the power exponent α and β. Therefore, the values of α and β were proposed to predict laminar flame speed of acetone/air in elevated temperature and pressure condition, which is the objective of the authors.

7. Reference

[1] K.-Y. Lam, W. Ren, S. H. Pyun, A. Farooq, D. F. Davidson and R. K. Hanson, "Multi-species time-history measurements during high-temperature acetone and 2-butanone pyrolysis," Proceedings of the Combustion Institute , vol. 34, no. 1, pp. 607-615, 2013.

[2] V. Robin, A. Mura, M. Champion, O. Degardin, B. Renou and M. Boukhalfa, "Experimental and numerical analysis of stratified turbulent V-shaped flames," Combustion and Flame , vol. 153, no. 1–2, pp. 288-315, 2008.

[3] A. Burluka, M. Harker, H. Osman, C. Sheppard and A. Konnov, "Laminar burning velocities of three C3H6O isomers at atmospheric pressure," Fuel , vol. 89, no. 10, pp. 2864-2872, 2010.

[4] E. Nilsson, L. de Goey and A. Konnov, "Laminar burning velocities of acetone in air at room and elevated temperatures," Fuel , vol. 105, no. 0, pp. 496-502, 2013.

[5] S. Pichon, G. Black, N. Chaumeix, M. Yahyaoui, J. Simmie, H. Curran and R. Donohue, "The combustion chemistry of a fuel tracer: Measured flame speeds and ignition delays and a detailed chemical kinetic model for the oxidation of acetone," Combustion and Flame , vol. 156, no. 2, pp. 494-504, 2009.

[6] C. T. Chong and S. Hochgreb, "Measurements of laminar flame speeds of acetone/methane/air mixtures," Combustion and Flame , vol. 158, no. 3, pp. 490-500, 2011.

[7] N. Bouvet, C. Chauveau, I. Gökalp, S.-Y. Lee and R. Santoro, "Characterization of syngas laminar flames using the Bunsen burner configuration," International Journal of Hydrogen Energy , vol. 36, no. 1, pp. 992-1005, 2011.

[8] A. Mazas, B. Fiorina, D. Lacoste and T. Schuller, "Effects of water vapor addition on the laminar burning velocity of oxygen-enriched methane flames," Combustion and Flame , vol. 158, no. 12, pp. 2428-2440, 2011.

[9] L. Selle, T. Poinsot and B. Ferret, "Experimental and numerical study of the accuracy of flame-speed measurements for methane/air combustion in a slot burner," Combustion and Flame , vol. 158, no. 1, pp. 146-154, 2011.

[10] M. Metghalchi and J. C. Keck, "Burning velocities of mixtures of air with methanol, isooctane, and indolene at high pressure and temperature," Combustion and Flame , vol. 48, no. 0, pp. 191-210, 1982.